

Size-Dependent Polar Ordering in Colloidal GeTe Nanocrystals

Mark J. Polking,[†] Jeffrey J. Urban,[‡] Delia J. Milliron,[‡] Haimei Zheng,^{§,||} Emory Chan,[‡] Marissa A. Caldwell,[⊥] Simone Raoux,[#] Christian F. Kieselowski,[§] Joel W. Ager, III,^{||} Ramamoorthy Ramesh,^{*,†,||} and A. Paul Alivisatos^{*,||,¶}

[†]Department of Materials Science and Engineering, University of California, Berkeley, Berkeley, California 94720, United States

[‡]The Molecular Foundry and [§]National Center for Electron Microscopy, Lawrence Berkeley National Laboratory, Berkeley, California 94720, United States

^{||}Department of Chemistry, University of California, Berkeley, Berkeley, California 94720, United States

[⊥]Department of Chemistry, Stanford University, Stanford, California 94305, United States

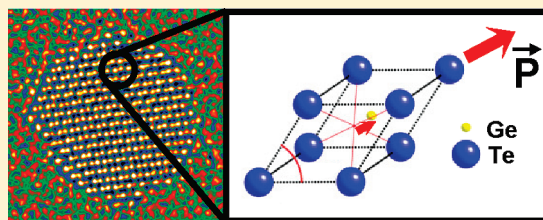
[#]IBM T. J. Watson Research Center, Yorktown Heights, New York 10598, United States

[¶]Materials Sciences Division, Lawrence Berkeley National Laboratory, Berkeley California 94720, United States

S Supporting Information

ABSTRACT: The question of the nature and stability of polar ordering in nanoscale ferroelectrics is examined with colloidal nanocrystals of germanium telluride (GeTe). We provide atomic-scale evidence for room-temperature polar ordering in individual nanocrystals using aberration-corrected transmission electron microscopy and demonstrate a reversible, size-dependent polar-nonpolar phase transition of displacive character in nanocrystal ensembles. A substantial linear component of the distortion is observed, which is in contrast with theoretical reports predicting a toroidal state.

KEYWORDS: Ferroelectric, nanocrystals, polar, colloidal, GeTe, phase transition



Ferroelectrics and related materials with a polar order parameter, or spontaneous electrical polarization, have attracted widespread interest for nonvolatile information storage devices, high- κ dielectrics, and many other applications.^{1,2} Practical applications of these materials, however, require room-temperature stability of the polar phase and a detailed understanding of polar ordering at the nanoscale. The fundamental nature of the polar state in low-dimensional nanomaterials has long remained a subject of controversy with conflicting literature reports indicating incoherent local polar distortions,^{3,4} the emergence of a toroidal polarization,^{5,6} or complete quenching of the polar state.^{7–9} In addition, while considerable attention has focused on perovskite thin films, the nature of polar ordering in other classes of ferroelectrics remains largely unexplored. Here, the size-dependent polar ordering in size-controlled nanocrystals of germanium telluride (GeTe), the simplest known ferroelectric, is examined in both ensembles and individual nanocrystals. We provide atomic-scale evidence of a room-temperature polar distortion retained at over 70% of the bulk value in nanocrystals less than 5 nm in size using aberration-corrected transmission electron microscopy (TEM) and detailed Rietveld refinement studies. In addition, we present temperature-resolved synchrotron diffraction and Raman spectroscopy studies demonstrating a reversible size-dependent polar phase transition. We find that the polar distortion retains significant linear, coherent character and arises via a polar phase transition that is displacive in nature, which is in contrast to theoretical reports⁶ suggesting a transition

to a toroidal state. The observed size-dependence of the polar ordering is attributed to surface-induced internal strains. This work demonstrates the surprising persistence of polar order at nanometer dimensions and provides an atomic-scale glimpse of polar ordering in a low-dimensional nanomaterial.

Germanium telluride has received much attention for its potential in phase-change memory devices,¹⁰ thermoelectrics,¹¹ and other applications. A semiconductor with a band gap of 0.1 eV in the bulk,¹² GeTe is also the simplest possible ferroelectric material,¹³ comprising one cation and one anion per primitive unit cell. Below ~ 625 K, the cubic rock salt lattice of GeTe undergoes a spontaneous symmetry-breaking distortion into a rhombohedral structure (space group $R3m$), which yields a polar phase.^{14,15} This distortion may be represented as an angular distortion of the unit cell with a concurrent displacement of the Ge sublattice,^{16,17} which generates a spontaneous polarization along a $[111]$ axis of the original cubic lattice (Figure 1).

This spontaneous polar ordering was probed using several different populations of monodisperse colloidal GeTe nanocrystals synthesized as described previously.¹⁸ Nanocrystals with average diameters of 8 and 17 nm were prepared by reaction of the divalent germanium precursor bis[bis(trimethylsilyl)amino]Ge(II) with trioctylphosphine-tellurium (TOP-Te).

Received: November 22, 2010

Revised: February 7, 2011

Published: February 21, 2011

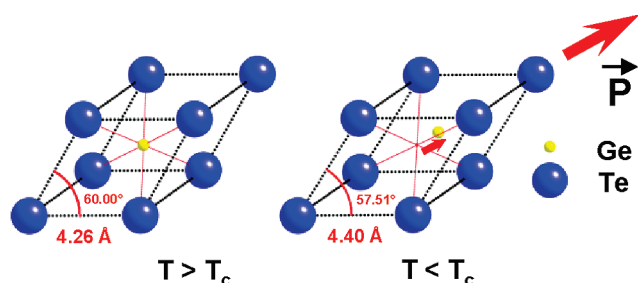


Figure 1. Schematic illustration of the spontaneous polar distortion in GeTe nanocrystals. The primitive unit cells for the cubic phase of GeTe (left), stable above ~ 625 K, and the low-temperature rhombohedral phase (right) are illustrated. The distortion results in a relative displacement of the Ge and Te sublattices that induces a spontaneous polarization (large red arrow) along a $[111]$ axis. The displacement of the Ge cation is exaggerated for clarity. (Structural parameters obtained from ref 16).

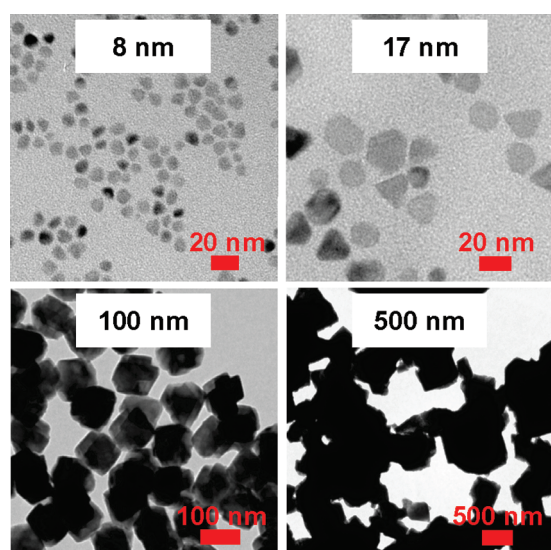


Figure 2. Transmission electron microscope images of the 8, 17, 100, and 500 nm GeTe nanocrystals studied. The size distributions for all syntheses were between 10 and 20%.

Nanocrystals with an average diameter of 100 nm were prepared by reaction of a precursor with slower nucleation kinetics, GeCl_2 -1,4 dioxane complex, with the same tellurium source. In addition, particles of ~ 500 nm average size were prepared as a reference sample by reaction of GeCl_2 -1,4 dioxane complex with TOP-Te at 300°C in the presence of oleylamine and oleic acid surfactants. Typical TEM images of these nanocrystals are shown in Figure 2.

Atomically resolved images of individual 4.5–8 nm GeTe nanocrystals provide direct evidence of the polar distortion in the smallest crystals synthesized (Figure 3 and Figures S1–S3, Supporting Information). Exit wave reconstructions of high-resolution TEM (HRTEM) focal series obtained with the aberration-corrected TEAM 0.5 and TEAM 1 microscopes conclusively demonstrate the existence of both the spontaneous angular distortion and sublattice displacement in nanocrystals less than 5 nm in diameter at room temperature. Fast Fourier transform (FFT) analysis of the reconstructed phase image of a single ~ 4.5 nm particle viewed along the $[100]$ zone axis (Figure 3a,b) illustrates an angular distortion of $\sim 1.1^\circ$. Lattices fit to the

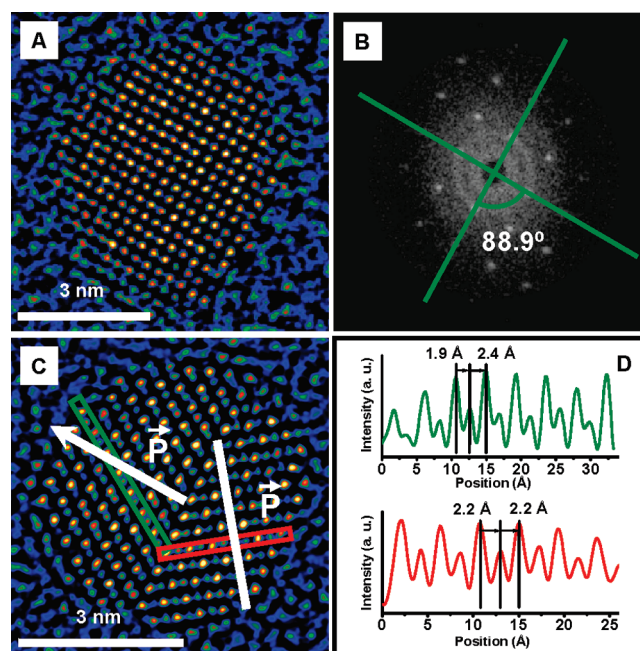


Figure 3. Atomically resolved polar distortion in individual colloidal GeTe nanocrystals. (A) Phase of the reconstructed electron exit wave for a single ~ 4.5 nm GeTe nanocrystal in the $[100]$ zone axis orientation. (B) Corresponding fast Fourier transform demonstrating an angular distortion of $\sim 1.1^\circ$. (C) Phase of the reconstructed electron exit wave of a single ~ 5 nm GeTe nanocrystal with a (111) twin boundary. (D) Corresponding line traces from the left (top) and right (bottom) sides. Separate Ge (smaller peaks) and Te (larger peaks) columns can be observed. The alternation of $\{111\}$ plane spacings arising from the Ge sublattice displacement is clearly apparent in the left section of the particle. No such staggering can be observed on the right side of the particle, consistent with a polarization vector in a (110) plane perpendicular to the viewing plane.

FFT of numerous particles using a least-squares procedure consistently indicated an angular distortion of $1\text{--}2^\circ$ with an error of approximately 0.5° (Supporting Information Figure S2), consistent with synchrotron X-ray diffraction data described below. Details of the analysis are provided in the Supporting Information. Analysis of reconstructed phase images also demonstrates the centrosymmetry-breaking sublattice displacement. A phase image of a ~ 5 nm nanocrystal containing a (111) twin boundary (Figure 3c, Supporting Information Figure S1) shows two distinct sections in a $[110]$ orientation with $\{111\}$ planes perpendicular to the viewing plane. Separate germanium and tellurium columns can be distinguished in the image, and a sublattice displacement, manifested in a staggering of the $\{111\}$ planes perpendicular to the polarization axis, measuring approximately 0.2 Å can be measured in the left section of the particle. This is reduced from the value of ~ 0.35 Å predicted theoretically.¹⁶ No such staggering can be observed in the right section, consistent with a polarization vector that lies in a (110) plane perpendicular to the viewing plane. Additional reconstructed phase images of GeTe nanocrystals in a $[110]$ orientation (Supporting Information Figure S3) indicate similar staggering of perpendicular $\{111\}$ planes. Moreover, these reconstructions are consistent with simulated phase images for a structure with a coherent sublattice displacement (Supporting Information Figure S3) generated using structural parameters from the literature.¹⁶ Although the exact nature of spatial correlations is

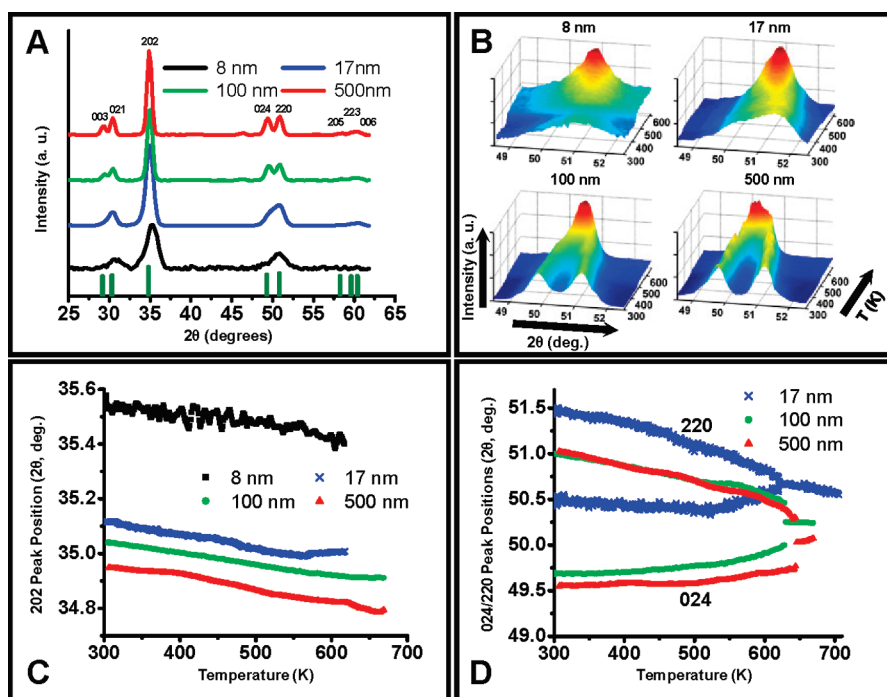


Figure 4. Temperature-dependent synchrotron X-ray diffraction studies of the polar phase transition in GeTe nanocrystals. (A) Room-temperature synchrotron powder X-ray diffraction patterns of GeTe nanocrystals. (B) Plots of diffracted intensity versus 2θ diffraction angle and temperature for the 024/220 doublet. Convergence of the doublet peaks into a single peak of higher intensity characteristic of the cubic phase can be seen with increasing temperature. (C) Position of the 202 (rhombohedral) diffraction peak as a function of temperature. (D) Peak positions of the 024/220 (rhombohedral) doublet peaks as a function of temperature. The room-temperature peak splitting decreases for smaller particle sizes, and the doublet collapses as the rhombohedral to cubic phase transition is approached.

Table 1. Structural Parameters for GeTe Nanocrystals Obtained by Rietveld Refinement of Room-Temperature Synchrotron X-Ray Diffraction Patterns^a

size (nm)	a (Å)	α (degrees)
8	5.93 ± 0.03	88.81 ± 0.02
17	5.96 ± 0.01	88.72 ± 0.01
100	6.017 ± 0.005	88.599 ± 0.004
500	6.023 ± 0.005	88.395 ± 0.005

^a A substantial reduction in the lattice constant is evident for the smallest nanocrystals. In addition, a monotonic increase in the rhombohedral angle is observed.

not entirely clear, these images demonstrate the persistence of a sizable coherent, linear component of the polar distortion, in contrast with literature reports indicating a transition to a toroidal state in both perovskite and GeTe nanodots.^{5,6}

The existence of a polar phase transition in ensembles of nanocrystals was subsequently confirmed by temperature-resolved synchrotron X-ray diffraction (Figure 4, Supporting Information Figure S4). The cubic-to-rhombohedral phase transition in GeTe splits each of the 111 and 220 diffraction peaks (of the cubic system) into distinct 003/021 (parent 111) and 024/220 (parent 220) rhombohedral doublets. This splitting provides a clear signature of the structural phase transition. Ensembles of GeTe nanocrystals were analyzed using synchrotron powder X-ray diffraction. The resulting patterns indicate the presence of phase-pure germanium telluride in the rhombohedral phase (Figure 4a). Analysis with Rietveld refinement (Table 1, Supporting Information Figure S5) indicates a monotonic increase in the rhombohedral angle (α) from 88.40 to 88.81° with

decreasing particle size, indicating >70% retention of the polar distortion down to dimensions of a few nanometers. In addition, the lattice constant (a) of the smallest (8 nm) nanocrystals (5.93 Å) is significantly reduced from the value of 6.023 Å found for the largest (500 nm) particles. The rhombohedral structural model consistently yielded a superior fit to the X-ray diffraction patterns for particles of all sizes, and the presence of an overall rhombohedral distortion in the smallest nanocrystals studied (8 nm) is further supported by our atomic-resolution TEM results indicating both an angular distortion of the cubic prototype lattice and a polar sublattice displacement.

Temperature ramps were then executed to follow the evolution of the 202 diffraction peak and of the 024/220 doublet. The 202 (rhombohedral) peak remains a singlet throughout the transition and may thus be used to monitor nanocrystallite size (Supporting Information Figure S6). Analysis of the phase transition was only considered for the 17, 100, and 500 nm particles for which little sintering occurs during the measurement (see Supporting Information). For all particle sizes, the peak position moved smoothly to smaller diffraction angle over the entire temperature range (Figure 4c, Supporting Information Figure S4). In addition, no discontinuity is evident near the expected phase transition temperature (~ 625 K), consistent with previous reports^{15,19} indicating a minimal volume change.

At room temperature, all nanocrystals exhibit splitting of the 024 and 220 diffraction peaks (Figure 4b,d) that decreases in magnitude for smaller particles, reflecting a reduced angular distortion. Upon heating, the splitting decreases monotonically for all sizes as the nanocrystals approach the cubic phase. For the 100 and 500 nm particles, the splitting collapses gradually at

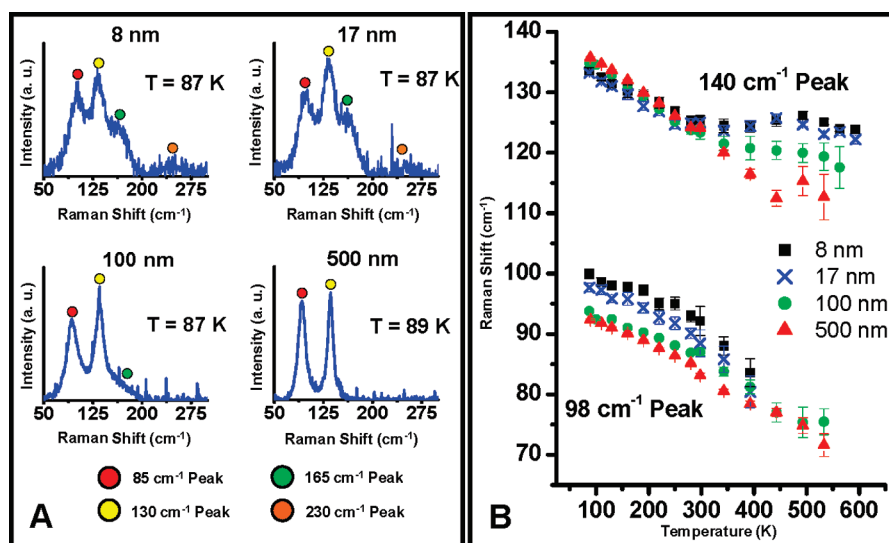


Figure 5. Temperature-dependent Raman scattering studies of GeTe nanocrystals. (A) Typical Raman spectra for films of 8, 17, 100, and 500 nm GeTe nanocrystals at ~ 87 K. All spectra contain strong peaks that can be assigned primarily to the A_1 and E symmetry optical phonon modes of crystalline GeTe. (B) Plot of the energies (in cm^{-1} units) of these two most prominent bands (primarily arising from the optical phonon modes of crystalline GeTe) as a function of temperature. Clear softening of both bands is observed for all particle sizes.

lower temperatures, then more rapidly near the expected phase transition temperature (~ 625 K). At higher temperatures, the doublet peaks can no longer be resolved, reflecting the structural transformation to the cubic phase. For the 17 nm particles the doublet collapses more smoothly over the entire temperature ramp with increasing rapidity starting as low as 425 K. Upon cooling, the doublets reappear, indicating recovery of the rhombohedral phase.

Further evidence of the displacive character of the phase transition was obtained through temperature-resolved Raman studies. Many materials with a displacive polar phase transition possess a “soft” zone-center optical phonon that decreases rapidly in energy as the phase transition temperature is approached.²⁰ In GeTe, the polar distortion splits a single triply degenerate Raman-inactive F_{1u} symmetry optical mode in the cubic structure into an A_1 symmetry transverse optical mode (~ 125 cm^{-1} at 300 K) and a doubly degenerate E symmetry transverse optical/longitudinal optical mode (~ 90 cm^{-1} at 300 K), both of which are Raman-active.²¹ The former (A_1) mode was determined to be the “soft” mode, and concurrent softening of the E symmetry mode was observed with increasing temperature. Since no Raman-active modes exist in the cubic-symmetry undistorted structure, the disappearance of these modes with increasing temperature and a pronounced decline in mode energies provide a spectroscopic signature of the phase transition.

Raman analyses of nanocrystal films (Figure 5, Supporting Information Figures S7 and S8) demonstrate clear mode softening characteristic of a displacive phase transition. The two most prominent peaks near 85 and 130 cm^{-1} in the spectra are assigned primarily to the two optical phonon modes of crystalline GeTe. Additional peaks of lower intensity around 165 and 230 cm^{-1} were observed in the spectra of the 8, 17, and 100 nm nanocrystals. We assign the additional modes to a contribution from a low-coordination surface layer (see Supporting Information).

Raman characterization of a reference sample of amorphous GeTe nanoparticles (Supporting Information Figure S9) revealed four peaks around 85, 125, 165, and 230 cm^{-1} , similar to the peak positions observed in the spectra of the 8, 17, and

100 nm particles.²² However, the band around 85 cm^{-1} is far more prominent for the crystalline samples, and the bands at 165 and 230 cm^{-1} become relatively weaker at progressively larger crystal sizes. The spectra of the nanocrystals can thus be understood as containing overlapping contributions from the crystalline interiors and low-coordination surfaces. The temperature dependencies of the positions and intensities of the 85 and 130 cm^{-1} features support this interpretation. While these peaks shift only a few wavenumbers (cm^{-1}) between 82 and 373 K for amorphous GeTe,²³ in crystalline GeTe their rapidly vanishing intensities and redshifts of tens of wavenumbers provide further support for observation of the displacive phase transition.²¹ For 100 and 500 nm nanocrystals, a rapid decline in the peak energies and the scattering intensities of the 85 and 130 cm^{-1} bands occurs with increasing temperature, indicative of the approaching phase transition. For the 8 and 17 nm nanocrystals, the 85 cm^{-1} band softens continuously from 87 through 400 K; however, the position of the 130 cm^{-1} band is stable above ~ 350 K. This is ascribed to a rapid decline in scattering intensity of the crystalline A_1 phonon approaching the phase transition, so that the weakly temperature-dependent contribution from the surface dominates at higher temperatures. The smooth softening of the phonon mode energies mirrors the smooth changes in structural distortion determined by the diffraction measurements and indicates significant retention of the displacive character of the phase transition down to nanometer dimensions.

The size effects observed throughout all experiments may be rationalized with a simple model based upon heightened surface-induced internal pressure. Several reports on nanosized perovskites implicate such internal strains in explaining reductions in the observed structural distortions and transition temperatures.^{7,24–26} A spherical particle of radius r with surface energy γ experiences an internal stress given by $p = 2\gamma/r$ that may be on the order of 10^8 – 10^{10} Pa for common values of surface energy.²⁴ Internal strains arising from free surfaces have been found to induce a phase transition from a tetragonal phase to a disordered cubic phase in isolated BaTiO_3 nanoparticles²⁵ and to suppress ferroelectric ordering in BaTiO_3 wires.²⁶ Phenomenological

modeling using Landau–Ginzburg–Devonshire theory by Morozovska et al. further indicates sizable shifts in bulk transition temperatures and suppression of ferroelectric ordering in spherical particles due to such surface stresses for positive values of the surface energy coefficient (i.e., compressive stress).²⁴ This result is consistent with our diffraction results, which indicate both a lattice contraction for the smallest particles and a monotonic decrease in the angular distortion as a function of particle size. Literature reports describe similar trends in GeTe under hydrostatic pressures of between 0 and 10 GPa,^{19,27,28} and transition pressures as low as 3.5 GPa have been reported for GeTe compressed in a solid medium.²⁷ Using the bulk modulus of GeTe reported in the literature ($K = 49.9$ GPa) as a guideline, we estimate an effective pressure of ~ 2.7 GPa for the 8 nm particles.¹⁹ These observations are also consistent with the Raman results, which indicate a $\sim 25\%$ reduction in the energy splitting of the E and A_1 symmetry peaks at low temperatures. The convergence of these peaks toward the triply degenerate F_{1u} mode of the cubic phase provides further evidence of the partial suppression of the polar distortion in the smallest particles. The temperature-dependence of the structural parameters is also consistent with this interpretation. Because of the reduced room-temperature structural distortions, it is anticipated that the temperature required to transform nanocrystals to the cubic phase would be reduced relative to bulk material. These trends are clearly manifest in the temperature-dependence of the 024/220 doublet peak positions. While the gradual nature of the change in angular distortion and the broadened peaks prevent an unambiguous identification of the size-scaling law governing the transition temperature, the collapse of the doublet at lower temperatures for smaller particles supports this interpretation.

The pronounced stability of the polar state may arise from screening of the polarization due to the high bulk conductivity of GeTe. Bulk GeTe contains Ge vacancies that lead to a high (10^{20} cm^{-3}) concentration of free holes.¹² At this carrier concentration, several free carriers are expected to be present in each nanocrystal, even for particles with an average diameter of 5 nm. These free carriers may screen induced surface charges and thereby minimize the depolarizing field. The stability of the polar state may also be attributable to effective compensation of polarization-induced surface charges by organic capping ligands.²⁹ These mechanisms are not reflected in theoretical calculations demonstrating vortex polarization states in GeTe,⁶ which may explain the discrepancy with our experiments.

This study provides atomic-scale evidence of the room-temperature stability of the polar phase in colloidal nanocrystals down to at least 5 nm in size and suggests the persistence of linear order at nanometer length scales. Synchrotron X-ray diffraction and Raman spectroscopy studies demonstrate a reversible polar-nonpolar phase transition leading to a size-dependent polar distortion that is displacive in nature, which has been directly confirmed with aberration-corrected transmission electron microscopy. This study reveals the surprising stability of polar distortions in freestanding nanometer-sized crystals and provides a platform for developing future fundamental studies of the nature of polar ordering at atomic length scales.

■ ASSOCIATED CONTENT

S Supporting Information. Full materials and methods, additional discussion, raw synchrotron X-ray and Raman

spectroscopy data. This material is available free of charge via the Internet at <http://pubs.acs.org>.

■ AUTHOR INFORMATION

Corresponding Author

*(R.R.) E-mail: rramesh@berkeley.edu. Phone: 510-642-2347.
(A.P.A.) E-mail: alivis@berkeley.edu. Phone: 510-486-5111.

■ ACKNOWLEDGMENT

The authors gratefully acknowledge Jonathan S. Owen and Dmitri V. Talapin for fruitful discussions and Bin Jiang for technical assistance. A portion of this work (synchrotron X-ray diffraction studies) was carried out by S.R. at the National Synchrotron Light Source, Brookhaven National Laboratory, which is supported by the U.S. Department of Energy, Division of Materials Sciences and Division of Chemical Sciences, under Contract No. DE-AC02-98CH10886. TEM studies were performed by M.J.P., H.Z., and C.F.K. at the National Center for Electron Microscopy, Lawrence Berkeley National Laboratory, which is supported by the Office of Science, Office of Basic Energy Sciences, of the U.S. Department of Energy under Contract No. DE-AC02-05CH11231. A portion of this work (analysis of synchrotron X-ray data, preparation of portions of the manuscript) was completed by J.J.U., D.J.M., E.C., and M.A.C. at the Molecular Foundry, Lawrence Berkeley National Laboratory, which is supported by the Office of Science, Office of Basic Energy Sciences, of the U.S. Department of Energy under Contract No. DE-AC02-05CH11231. All other work (synthesis, Raman studies, preparation of most of the manuscript) completed by M.J.P. with assistance from J.W.A., R.R., and A.P.A. was supported by the Physical Chemistry of Nanocrystals Project of the Director, Office of Science, Office of Basic Energy Sciences, Materials Sciences and Engineering Division, of the U.S. Department of Energy under Contract No. DE-AC02-05CH11231. M.J.P. was supported by a National Science Foundation Graduate Research Fellowship and by a National Science Foundation Integrative Graduate Education and Research Traineeship (IGERT) fellowship.

■ REFERENCES

- (1) Scott, J. F.; Paz de Araujo, C. A. *Science* **1989**, *246*, 1400.
- (2) Scott, J. F. *Science* **2007**, *315*, 954.
- (3) Smith, M. B.; Page, K.; Siegrist, T.; Redmond, P. L.; Walter, E. C.; Seshadri, R.; Brus, L. E.; Steigerwald, M. L. *J. Am. Chem. Soc.* **2008**, *130*, 6955.
- (4) Petkov, V.; Gateshki, M.; Niederberger, M.; Ren, Y. *Chem. Mater.* **2006**, *18*, 814.
- (5) Naumov, I. I.; Bellaiche, L.; Fu, H. *Nature* **2004**, *432*, 737.
- (6) Durgun, E.; Ghosez, P.; Shaltaf, R.; Gonze, X.; Raty, J.-Y. *Phys. Rev. Lett.* **2009**, *103*, No. 247601.
- (7) Uchino, K.; Sadanaga, E.; Hirose, T. *J. Am. Ceram. Soc.* **1989**, *72*, 1555.
- (8) Chattopadhyay, S.; Ayyub, P.; Palkar, V. R.; Multani, M. *Phys. Rev. B* **1995**, *52*, 13177.
- (9) Zhong, W. L.; Wang, Y. G.; Zhang, P. L.; Qu, B. D. *Phys. Rev. B* **1994**, *50*, 698.
- (10) Wuttig, M.; Yamada, N. *Nat. Mater.* **2007**, *6*, 824.
- (11) Snyder, J.; Toberer, E. S. *Nat. Mater.* **2008**, *7*, 105.
- (12) Chopra, K. L.; Bahl, S. K. *J. Appl. Phys.* **1970**, *41*, 2196.
- (13) Lines, M. E.; Glass, A. M. *Principles and Applications of Ferroelectrics and Related Materials*; Clarendon Press: Oxford, 1977; pp 519–524.

- (14) Rabe, K. M.; Joannopoulos, J. D. *Phys. Rev. B* **1987**, *36*, 6631.
- (15) Chattopadhyay, T.; Boucherle, J. X.; Von Schnering, H. G. *J. Phys. C: Solid State Phys.* **1987**, *20*, 1431.
- (16) Lencer, D.; Salinga, M.; Grabowski, B.; Hickel, T.; Neugebauer, J.; Wuttig, M. *Nat. Mater.* **2008**, *7*, 972.
- (17) Goldak, J.; Barrett, C. S.; Innes, D.; Youdelis, W. J. *Chem. Phys.* **1966**, *44*, 3323.
- (18) Polking, M. J.; Zheng, H.; Ramesh, R.; Alivisatos, A. P. *J. Am. Chem. Soc.* **2011** in press.
- (19) Onodera, A.; Sakamoto, I.; Fujii, Y.; Mori, N.; Sugai, S. *Phys. Rev. B* **1997**, *56*, 7935.
- (20) Scott, J. F. *Rev. Mod. Phys.* **1974**, *46*, 83.
- (21) Steigmeier, E. F.; Harbeke, G. *Solid State Commun.* **1970**, *8*, 1275.
- (22) Caldwell, M. A.; Raoux, S.; Wang, R. Y.; Philip Wong, H.-S.; Milliron, D. J. *J. Mater. Chem.* **2010**, *20*, 1285.
- (23) Andrikopoulos, K. S.; Yannopoulos, S. N.; Voyiatzis, G. A.; Kolobov, A. V.; Ribes, M.; Tominaga, J. *J. Phys.: Condens. Matter* **2006**, *18*, 965.
- (24) Morozovska, A. N.; Glinchuk, M. D.; Eliseev, E. A. *Phys. Rev. B* **2007**, *76*, No. 014102.
- (25) Shiratori, Y.; Pithan, C.; Dornseiffer, J.; Waser, R. *J. Raman Spectrosc.* **2007**, *38*, 1288.
- (26) Geneste, G.; Bousquet, E.; Junquera, J.; Ghosez, P. *Appl. Phys. Lett.* **2006**, *88*, No. 112906.
- (27) Kabalkina, S. S.; Vereshchagin, L. F.; Serebryanaya, N. R. *Sov. Phys. JETP* **1967**, *24*, 917.
- (28) Ciucivara, A.; Sahu, B. R.; Kleinman, L. *Phys. Rev. B* **2006**, *73*, No. 214105.
- (29) Spanier, J. E.; Kolpak, A. M.; Urban, J. J.; Grinberg, I.; Ouyang, L.; Yun, W. S.; Rappe, A. M.; Park, H. *Nano Lett.* **2006**, *6*, 735.